Development of a Low-cost Automated Micro Dispense Digital Goniometric Device with Drop Shape Analysis

R.M.D.M. Senarathna, W.K.I.L. Wanniarachchi and S. Jayawardhana
Dept. of Physics
University of Sri Jayewardenepura
Nugegoda, Sri Lanka
sasanijay@sci.sjp.ac.lk

D.R. Rathnaweera
Dept. of Chemistry
University of Sri Jayewardenepura
Nugegoda, Sri Lanka

***Abstract*—Accurate measurement of contact angles can define fluid dynamics, surface material properties and contribute to the development of micro/nanofluidic devices. The drop shape analysis technique was developed to accurately determine the contact angle and surface tension of a liquid drop on a solid surface. The technique involves capturing a reflected image of the drop profile, acquiring coordinate points along the contour and finding the mathematical best-fit accordingly. Many conventional equipment utilizes this method through manual acquisition and analysis of data. This is an arduous, time consuming task which can introduce inaccuracies. Nevertheless, partially automated equipment can be prohibitively expensive. Here its shown that by utilizing embedded system development techniques, both the imaging and profile analyzing tasks as well as the liquid dispenser can be automated and precisely controlled by a computer application at a fraction of the cost of a commercial unit. The developed system also facilitates sample stage tilting which can provide information on dynamic liquid profiles to determine advancing and receding contact angles. Importantly the device is capable of dispensing and analyzing less than 5 nl volumes of liquid. Such measurements are becoming increasingly important in the understanding of areas such as superhydrophobicity and microfluidic devices.**

Keywords—goniometer; contact angles; sessile drop method; drop shape analysis; suerhydrophobicity

I. Introduction

During the past decade, studies of surface wettability has increased rapidly [1-3]. A thorough understanding of surface wettability is important in both fundamental and applied viewpoints. Recently, these have further extended to the study of superhydrophobicity, a phenomenon which is reported to exhibit self-cleaning properties [4], drag reduction [5], electrowetting [6] etc. Contact angle measurement plays a vital role in determining surface wettability, surface energy and surface tension of various liquids. Contact angle measuring methods can be divided into two categories; tensiometry and goniometry. The tensiometry method utilizes the Young-Laplace equation [7] to determine the contact angle by measuring interactive forces between the solid-liquid interface. Goniometry is an optical method which involves capturing a high-contrast image of the liquid droplet on a target surface and directly measuring the contact angle of the solid-liquid-air triple point.

Nevertheless, the measurements made by the tensiometry method, can be affected by line tension [8], electrostatic potential [9], surface roughness [10], and external forces, which do not play a role in the goniometry method. Another important aspect of using goniometry method is the study of contact angles of dynamic liquid droplets [11].

In their work Benoit et al. [12] presented a precise goniometer using a low-cost single board computer. The work used a charge coupled device (CCD) camera to capture an image of a back-illuminated water drop on a target surface (Sessile drop). A solution based on the Young-Laplace equation has been fitted to the acquired drop profile and the surface tension and contact angle were determined using pendant drops and sessile drops. Despite the promising results, the system was lacking the automated control provided in most commercial units. Most low-cost contact angle measuring devices are only capable of measuring static contact angles [12,13]. Whereas, Kwok et al. [14] had described the importance of dynamic contact angle measurements for distinguishing between good and bad contact angles.

In this work, a low-cost automated Drop Shape Analyzer (DSA) is presented. The device is capable of conducting multiple analysis which includes, static contact angle measurement of a sessile drop and dynamic contact angle measurement by both the tilting cradle method and drop inflation/deflation method. If required, pendant drop analysis can also be conducted by the same apparatus. The novelty of the apparatus lies in its ability to achieve less than 5 nl dispensing accuracy, while maintaining the advanced functionality of a commercially available DSA device at a fraction of its cost. Such system enables the study of micro/nano fluidic behavior, the understanding of which is vital in developing superhydrophobic surfaces and micro-fluidic devices.

II. Implementation

The measurement of contact angle using the sessile drop method involves dispensing a predefined volume of liquid on to the test surface, capturing an image along the cross section of the droplet, analyzing the drop shape and determining the contact angle. The measurement of the dynamic contact angles involve an additional step of sample tilting. Therefore, the experimental setup involves four main stages; a micro syringe control mechanism, a sessile drop image

978-1-5386-4417-1/18/$31.00

capturing stage, a sample stage tilting mechanism and an image processing/analyzing stage using a custom coded computer application.

A. Micro Syringe Control Mechanism

This stage of the device is responsible for delivering a user specified volume of liquid to the dispensing needle to form a liquid drop for analysis. This is done by using a precision micro syringe and controlling the syringe plunger electromechanically to increase accuracy and precision of the liquid delivery (Fig. 1). The glass micro syringe used in this experiment consist of a 100 microliter graduated reservoir with a stainless steel plunger and a needle. Dispensing of microliter scale volumes were achieved by controlling the linear motion of the plunger using a custom built linear actuator including a stepper motor driven by an Arduino Mega microcontroller board combined with a stepper motor driver board (Fig. 2). Alternatively, a Raspberry Pi could be used for a portable unit. Nevertheless, the Arduino and PC combination provides a much user-friendly lab-based set-up which enables non-experts to perform measurements and further analysis. The linear actuator was made out of a threaded rod driven through a nut connected to a couple of bearing blocks on two stainless steel linear rails. The dispenser setup and the sample stage were physically separated using an elongated clear dispenser tube. This was done in order to isolate the vibrations from the stepper motor device being transferred to the droplet. The minimum volume that can be dispensed by this method was expected to be less than 5 nl. Although picoliter dispense volumes can be achieved with piezo-electrical actuators which are mostly used for bio-medical applications. [15] On the other hand, such systems require advanced cameras and high-end optics which would drastically increase the price of such unit. A typical DSA's used for standard applications would have a minimum dispense volume of 100 nl. [16]

All mechanical components were mounted on aluminium cladding panels using stainless steel screws or nuts and bolts. Instructions for driving the stepper motor was fed through from the PC (personal computer) application software to the Arduino microcontroller board via a USB (Universal Serial Bus) interface.

B. Sessile Drop Image Capturing

This stage includes, an LED (light emitting diode) panel light, microscope CCD camera with USB connectivity and the sample stage in between them. The microscope CCD camera is pointed at the liquid drop on the sample stage and the drop is illuminated from behind by the LED panel light to create a high-contrast shadow image of the drop (Fig. 3).

C. Sample Stage Tilting Mechanism

This allows the device to manipulate the sessile drop shape by changing the horizontal angle of the sample stage. This was achieved by a stepper motor connected to the sample stage using a belt and pulley system. As before, the stepper motor was controlled by the same Arduino microcontroller board combined with a separate stepper motor driver board (Fig. 2). The instructions needed to drive the stepper motor was generated by the same PC application software. To measure the tilt angle, an ADXL345 triple-axis accelerometer was securely placed inside the sample stage and connected to the microcontroller board for data acquisition and transmission to the computer application. The sample stage is capable of tilting a secured sample surface up to an angle of 90° in both directions.

D. Image Processing

In this stage the captured image was converted to an 8-bit grayscale format for faster analysis. The PC application software was written in C# while utilizing the AForge.NET version 2.2.5 C# libraries as the image processing framework. The software is also responsible for controlling all electromechanical components and sensors by providing instructions to the Arduino microcontroller board via the USB interface.

1) Grayscale conversion: Fig. 3 shows a sessile drop captured by the microscope CCD camera. Even though the color image captured by the camera was similar to a grayscale image, it was converted to a proper grayscale image using image manipulation methods provided by the AForge.NET libraries. This way, each pixel will have a single 8-bit intensity value which will make the image more suitable for the edge detection algorithm.

2) Edge detection: Edge detection algorithm performs horizontal pixel sweeps upwards starting from the user defined base line (solid-liquid interface), during the sweep it captures and saves the 2 dimensional coordinate at the point where the predefined threshold intensity change occurs (Fig. 3). The device is capable of acquiring up to a maximum of 100 edge coordinates, which is a user defined value.

E. Data Analysis

In this stage of the experiment, the application uses the results from edge detection to make separate coordinate arrays for both left and right sides of the drop contour. After the data has been acquired, mathematical formula fitting and contact angle calculation can be performed. The algorithms and methods to perform those tasks were also developed utilizing Visual Studio 2015 Community edition IDE and Visual C# language package.

1) Mathematical Formula Fitting: The data array from the edge detection was used as data points for the mathematical formula fitting. The multiple order polynomial fitting method was used to generate the curves for the two sides of the drop separately. The polynomial is in the form of,

$$f(x) = \sum_{i=0}^{N} a_i x_i \tag{1}$$

where N is the order of the polynomial, x is the x-coordinate of any data point and a is a constant parameter. This fitting method is widely used for its proven reliability over an extended range of contact angles [17]. Therefore, this method was used to maintain the industry standard. The formula fitting was done using the least-square algorithm provided by MathNet.Numerics version 3.13.1 package for Visual C#. Although a standard image processing software toolbox would provide this technique, a customized software was developed using open source software as an integrated system while reducing the overall cost.

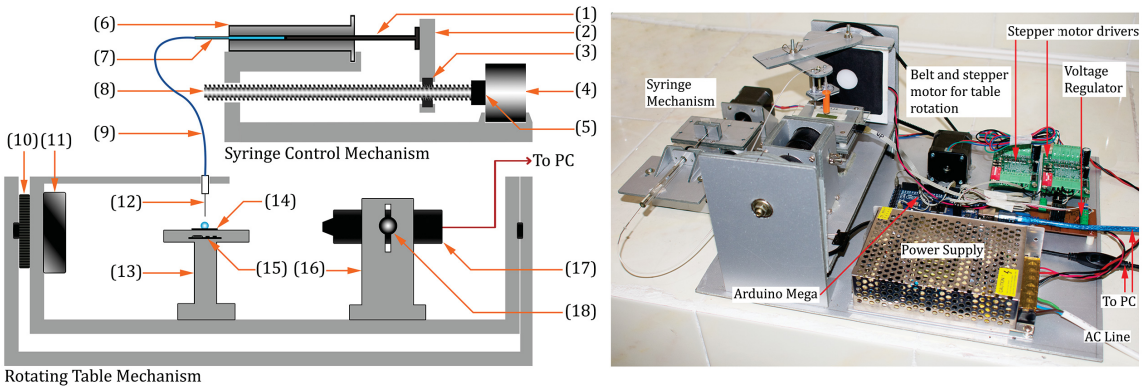

Fig. 1. Detailed schematic diagram of the DSA (Left): (1) micro syringe plunger, (2) plunger control arm, (3) hex nut, (4) stepper motor, (5) motor shaft coupler, (6) micro syringe, (7) micro syringe needle, (8) threaded rod, (9) 0.5 mm clear tube, (10) pulley for timing belt, (11) LED diffuse light, (12) smaller syringe needle, (13) sample table, (14) sample substrate, (15) digital accelerometer, (16) CCD camera holder, (17) microscope CCD camera, (18) camera angle retention screw. and photograph of the complete setup(Right).

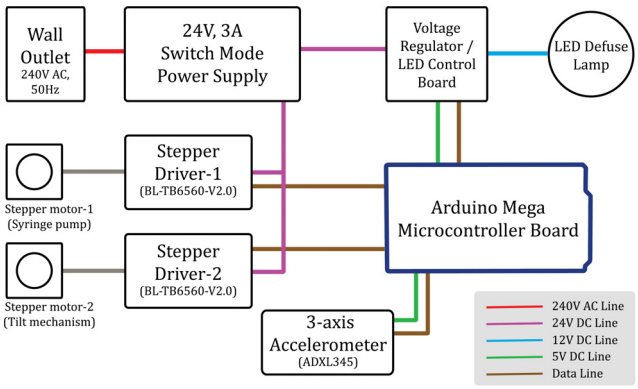

Fig. 2. Schematic of the controlling electronics.

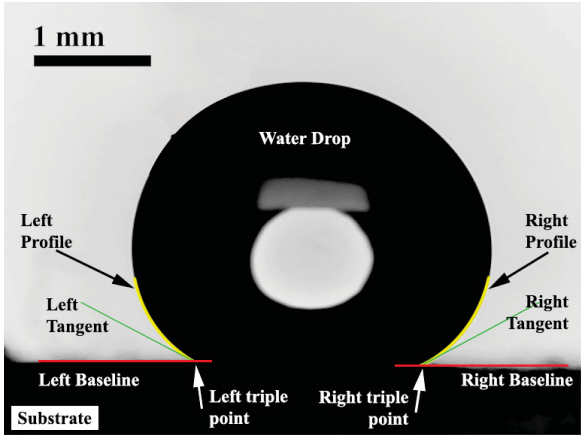

Fig. 3. Image of sessile drop captured by the microscope CCD camera.

2) Contact Angle Calculation: Once optimum parameters for the formula were generated for each side, its gradient function was calculated using the first derivative,

$$g(x) = \frac{d}{dx} f(x) \tag{2}$$

This can be used to calculate left contact angle,

$$\theta_L = tan^{-1} g(x_L) \tag{3}$$

and right contact angle,

$$\theta_R = 180 - tan^{-1} g(x_R) \tag{4}$$

where x_L and x_R are left and right triple point x-coordinates respectively.

III. Static and Dynamic Contact Angle Measurements

A. Static Contact Angle

Static contact angles are measured when the liquid drop is in an equilibrium state. Usually the sample stage is kept perfectly horizontal, thus producing an axisymmetric drop profile for homogeneous surfaces. The DSA's sample stage tilt mechanism was used to rotate the sample stage with a precision of 0.03^o and on-screen display was used to monitor the said angle. This precision was acquired by careful calibration of stepper motor and timing belt system. The accelerometer was mainly used for detecting the horizontal position of the sample stage.

In this work, five different sample surfaces were used to measure static contact angle with distilled water (Table I). To evaluate the accuracy of the DSA, the results were compared against two contact angle measuring applications; DropSnake and LB-ADSA (Low Bond Axisymmetric Drop Shape Analysis). These two methods come as plugins for ImajeJ 1.51j8 version which is freely distributed over the internet. DropSnake can be applied to both axisymmetric and asymmetric drop profiles while LB-ADSA only supports axisymmetric drop profiles. Since the horizontal sample stage arrangement helps to create axisymmetric drop profiles, The DSA contact angles were compared against both DropShape and LB-ADSA methods.

B. Dynamic Contact Angle

Dynamic contact angles are determined in the course of wetting and dewetting of a particular surface by a liquid.

TABLE I. SAMPLE SURFACES USED TO MEASURE STATIC CONTACT ANGLE OF DISTILLED WATER AND THEIR EXPECTED CONTACT ANGLE RANGES

No.	Sample Surface	Expected CA range
1	Smooth glass surface	$20^\circ - 60^\circ$
2	Polycarbonate sheet	$60^\circ - 80^\circ$
3	Flat polydimethylsiloxane surface	$80^\circ - 100^\circ$
4	Hydrophobic spray coated fabric	$100^\circ - 150^\circ$
5	Top surface of Taro (*Colocasia esculenta*) leaf	more than150°

Advancing and receding contact angles are measured respectively in each state of the drop. Wetting and dewetting of a surface can be accomplished by either of two methods; inflation/deflation and sample stage tilting (also known as tilting cradle method). The DSA presented in this work is capable of performing both techniques.

1) Inflation/deflation method: This is done by using the syringe control mechanism to control the volume of liquid that is supplied or withdrawn from the drop, causing it to inflate or deflate. Advancing angle is the maximum contact angle generated when inflating the liquid drop on target surface without an increase in the solid-liquid interfacial area. Similarly, receding angle is the minimum contact angle generated when deflating the liquid drop on the target surface without a decrease in the solid-liquid interfacial area.

To find the dynamic contact angles using this technique, the DSA was configured to automatically inflate a drop on a target surface up to a certain defined volume and then deflate it back to the original volume while capturing images after each inflation or deflation. In order to ascertain the validity of the procedure, a polycarbonate surface and dehydrated Taro leaf surface were tested. Since the inflation/deflation method was performed by keeping the sample stage horizontal, it was noted that axisymmetric drop profiles occur, thus enabling the use of any one of above mentioned 3 types of contact angle determination methods.

2) Tilting Cradle Method: Here we used the motorized rotation of the sample stage to manipulate the drop status and create dynamic liquid drop conditions on the target surface. When increasing the horizontal angle of the sample stage, gravitational force that was acting on the liquid's center of mass shifts to one side and creates a deformed, asymmetric drop profile to compensate the change. If the tilting angle continued to increase, at a certain angle the drop will disengage from the surface and travel down the slope. This critical horizontal angle is called sliding angle. The maximum and minimum contact angles of the drop at this point are defined as dynamic contact angles (i.e. advancing contact angle and receding contact angle respectively).

To determine the dynamic contact angles using this technique, the DSA was configured to automatically rotate the sample stage up to a certain user-defined angle while capturing images after each rotation step of the stage. The validation of the procedure was tested for two surfaces; a polycarbonate surface and a flat PDMS (polydimethylsiloxane) surface. This technique creates asymmetric drop profiles, thus making the LB-ADSA method useless here. But the DSA results can be compared against DropSnake results.

Final data of both techniques can be exported as separate images for each step and contact angles as a Microsoft Excel workbook.

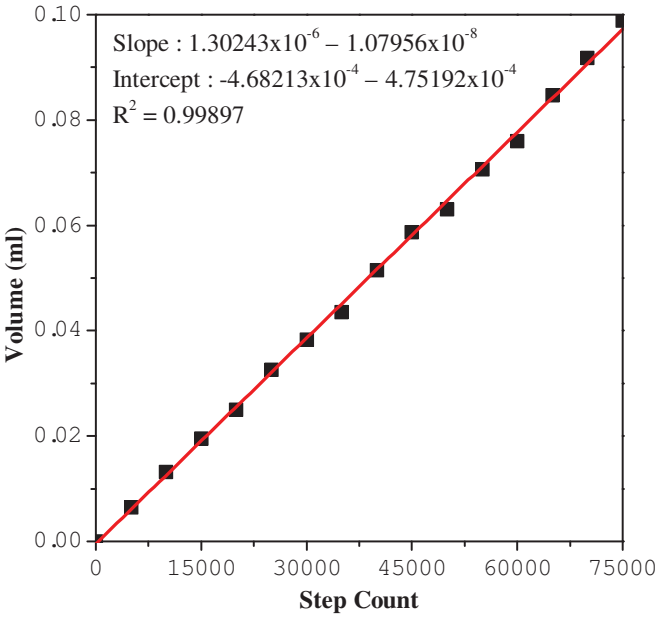

Fig. 4. Amount of stepper motor steps required to deliver a certain volume of liquid.

IV. RESULTS AND DISCUSSION

A. Volume Dispense Accuracy

Accuracy of the volume dispenser of the micro syringe mechanism is shown in Fig. 4. The theoretical minimum volume which can be dispensed was calculated to be 1.302 ± 0.001 nl (per step). However, the practical minimum volume was configured to be 5.0 ± 0.2 nl for ease of use.

B. Static Contact Angle

Table II shows results obtained for static contact angles of distilled water for different surfaces (listed in Table I) by different methods. Methods such as DropSnake involves manual selection of points which introduces human errors. On the other hand, LB-ADSA uses Young-Laplace fit which takes surface energy into account [18] and is particularly suited for contact angle measurements. The maximum error between the LB-ADSA method and this solution based on these data is 6.5% for the near 90° measurements. For all other surfaces including superhydrophobic surfaces, the error remained below 2.5%. The reason for the higher error percentage for near normal contact angles could be attributed to the difficulty in fitting a polynomial at that angle. Nevertheless, further processing could easily remove this inaccuracy. [19]

It is also important to mention the time taken for each method for a single measurement; DropSnake plugin fitting took 30 ± 5 seconds, while LB-ADSA consumed 60 ± 10 seconds to fit a single curve to a drop profile and measure contact angles. In contrast, DSA only took less than 500 milliseconds to perform the same task.

TABLE II. STATIC CONTACT ANGLES OF WATER ON DIFFERENT SURFACES OBTAINED BY DSA, LB-ADSA AND DROPSNAKE METHODS. EACH DATA POINT IS AN AVERAGE OVER 5 DIFFERENT FITTING ATTEMPTS.

Surface No.	DSA			DropSnake			LB-ADSA
	CA_L	*CA_R*	*CA_Avg*	*CA_L*	*CA_R*	*CA_Avg*	*CA_Avg*
1	$50.5^\circ \pm 0.3^\circ$	$54.0^\circ \pm 0.1^\circ$	$52.3^\circ \pm 0.1^\circ$	$51.9^\circ \pm 0.3^\circ$	$48.8^\circ \pm 0.3^\circ$	$50.4^\circ \pm 0.2^\circ$	$53.2^\circ \pm 0.3^\circ$
2	$82.4^\circ \pm 0.1^\circ$	$79.1^\circ \pm 0.4^\circ$	$80.8^\circ \pm 0.2^\circ$	$75.7^\circ \pm 0.3^\circ$	$72.1^\circ \pm 0.5^\circ$	$73.9^\circ \pm 0.4^\circ$	$81.9^\circ \pm 0.4^\circ$
3	$89.9^\circ \pm 0.6^\circ$	$89.5^\circ \pm 0.3^\circ$	$89.7^\circ \pm 0.4^\circ$	$85.5^\circ \pm 0.4^\circ$	$86.3^\circ \pm 0.4^\circ$	$85.9^\circ \pm 0.3^\circ$	$94.7^\circ \pm 0.4^\circ$
4	$129.1^\circ \pm 0.8^\circ$	$123.9^\circ \pm 0.9^\circ$	$126.5^\circ \pm 0.3^\circ$	$122.3^\circ \pm 0.4^\circ$	$121.9^\circ \pm 0.2^\circ$	$122.1^\circ \pm 0.3^\circ$	$127.3^\circ \pm 0.5^\circ$
5	$163.0^\circ \pm 0.7^\circ$	$153.8^\circ \pm 0.6^\circ$	$158.4^\circ \pm 0.7^\circ$	$155.9^\circ \pm 0.4^\circ$	$146.6^\circ \pm 0.4^\circ$	$151.3^\circ \pm 0.2^\circ$	$156.4^\circ \pm 0.6^\circ$

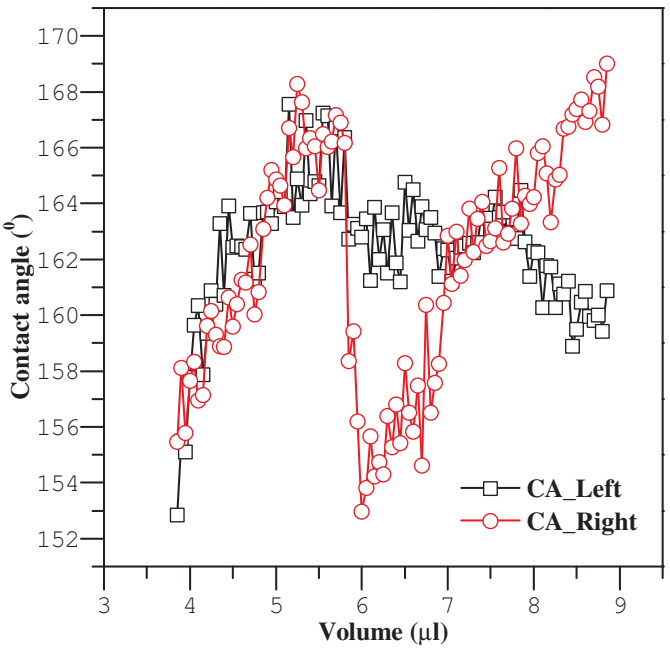

Fig. 5. Dynamic water contact angles on a dehydrated Taro leaf substrate.

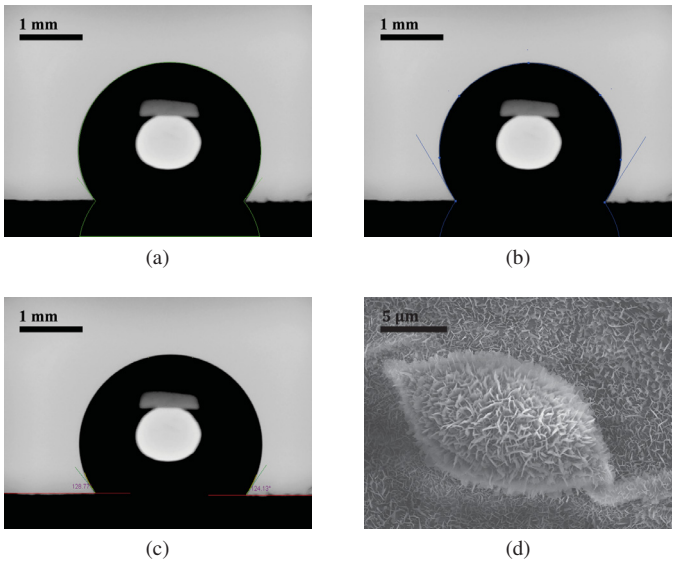

(a) (b) (c) (d)

Fig. 6. Static contact angle of water on dehydrated Taro leaf substrate obtained by: (a) LB-ADSA, (b) DropSnake, (c) DSA using same drop image and (d) scanning electron microscope image of a micro-structure on the dehydrated Taro leaf.

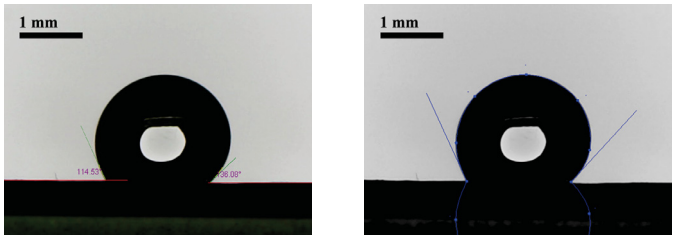

(a) (b)

Fig. 7. Contact angles of water drop on a tilted substrate of dehydrated Taro leaf measured using: (a) DSA, (b) DropSnake.

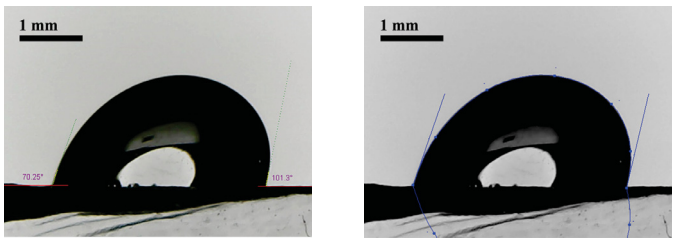

(a) (b)

Fig. 8. Contact angles of water drop on a tilted substrate of flat PDMS measured using: (a) DSA, (b) DropSnake.

C. Dynamic Contact Angles

Fig. 5 shows results of automated inflation/deflation method to find advancing and receding contact angles. The amount of noise in the data is caused by the non-uniformity of the target surface and small vibrations. It is clear that the left and right contact angles are not uniform according to the graph. Which shows the unpredictable behavior of a dynamic water droplet on a rough micro-patterned surface. However, in the wetting procedure (inflating), the maximum angle of the data set was considered to be the advancing angle, which can be clearly noticed in the Fig. 5. The fluctuations in the pattern can be explained through the expansion of the drop's solid-liquid interfacial area [20] over a micro-patterned surface. The Taro leaf is known to contain a micro/nano-patterned surface which cause it to exhibit superhydrophobic properties (see Fig. 6d). Fig. 7 and Fig. 8 show images of water drops on two different surfaces taken during tilting cradle method to find dynamic contact angle and sliding angle. Since the drops have asymmetric profiles LB-ADSA method cannot be used in this instance to measure contact angles. DSA contact angles were only compared against DropSnake contact angles.

Fig. 9 illustrates the usage of automated contact angle measurements coupled with sample stage tilting mechanism. This enables the user to study this kind of dynamic drop behavior more efficiently.

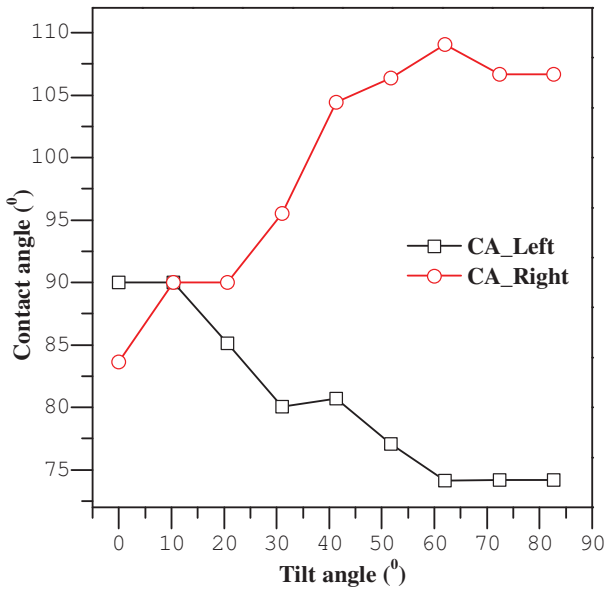

Fig. 9. Contact angles of a water drop on a textured PDMS substrate with sample stage angle.

V. Conclusion

Micro syringe control mechanism with precision drop shape analysis allow users to obtain highly detailed dynamic contact angle data with the developed DSA unit. DSA's results for contact angles between 20° and 170° are reliable considering the cost of development. Comparing to other low-cost contact angle determination techniques (i.e. DropSnake, LB-ADSA) DSA is much faster and easy to use. The developed DSA unit is capable of measuring; static, advancing, receding and sliding contact angles down to sub-microliter volumes.

Acknowledgment

The authors would like to thank the Center for Advanced Material Research at University of Sri Jayewardenepura (Grant No AMRC/RE/2016/M.Phil-04) for the funding support and Sri Lanka Institute of Nanotechnology for the scanning electron microscope (SEM) images.

References

[1] J. Wei, T. Igarashi, N. Okumori, T. Igarashi, T. Maetani, B. Liu, and M. Yoshinari. (2009, Jun.) "Influence of surface wettability on competitive protein adsorption and initial attachment of osteoblasts." *Biomedical Materials*. [On-line]. 4(4). p. 045002. Available: http://stacks.iop.org/BMM/4/045002 [Oct. 20, 2017].

[2] J. Wu, T. Yi, T. Shu, M. Yu, Z. Zhou, M. Xu, Y. Zhou, H. Zhang, J. Han, F. Li, and C. Huang. (2008, Dec.) "Ultrasound switch and thermal self-repair of morphology and surface wettability in a cholesterol-based self-assembly system." *Angewandte Chemie*. [On-line]. 120(6). pp. 1079–1083. Available: https://onlinelibrary.wiley.com/doi/abs/10.1002/anie.200703946 [Oct. 20, 2017].

[3] J. S. Coursey and J. Kim. (2008, Dec.) "Nanofluid boiling: The effect of surface wettability." *International Journal of Heat and Fluid Flow*. [On-line]. 29(6). pp. 1577–1585. Available: https://www.sciencedirect.com/science/article/pii/S0142727X08001227 [Oct. 20, 2017].

[4] R. Furstner, W. Barthlott, C. Neinhuis, and P. Walzel, "Wetting and self-cleaning properties of artificial superhydrophobic surfaces," *Langmuir*, vol. 21, pp. 956–961, Jan. 2005.

[5] R. J. Daniello, N. E. Waterhouse, and J. P. Rothstein. (2009, Aug.) "Drag reduction in turbulent flows over superhydrophobic surfaces." *Physics of Fluids*. [On-line]. 21(8). p. 085103. Available: https://aip.scitation.org/doi/10.1063/1.3207885 [Oct. 20, 2017].

[6] F. Lapierre, Y. Coffinier, R. Boukherroub, and V. Thomy. (2013, Oct.) "Electro-(de)wetting on superhydrophobic surfaces." *Langmuir*. [On-line]. 29(44). pp. 13 346–13 351. Available: https://pubs.acs.org/doi/full/10.1021/la4026848 [Oct. 20, 2017].

[7] A. W. Adamson and A. P. Gast, *Physical chemistry of surfaces*. Wiley-Interscience publication, New York, 1967, pp. 6–7.

[8] A. Marmur. (1997, Feb.) "Line tension and the intrinsic contact angle in solidliquidfluid systems." *Journal of Colloid and Interface Science*. [On-line]. 186(2). pp. 462–466. Available: https://www.sciencedirect.com/science/article/pii/S0021979796946664 [Oct. 20, 2017].

[9] K. H. Kang. (2002, Nov.) "How electrostatic fields change contact angle in electrowetting." *Langmuir*. [On-line]. 18(26). pp. 10 318–10 322. Available: https://doi.org/10.1021/la0263615 [Jan. 10, 2018].

[10] R. N. Wenzel, "Surface roughness and contact angle." *The Journal of Physical and Colloid Chemistry*, vol. 53(9), pp. 1466–1467, Sep. 1949.

[11] C. Lam, R. Ko, L. Yu, A. Ng, D. Li, M. Hair, and A. Neumann. (2001, Nov.) "Dynamic cycling contact angle measurements: Study of advancing and receding contact angles." *Journal of Colloid and Interface Science*. [On-line]. 243(1). pp. 208–218. [Jan. 15, 2018].

[12] B. Favier, N. T. Chamakos, and A. G. Papathanasiou. (2017, Nov.) "A precise goniometer/tensiometer using a low cost single-board computer." *Measurement Science and Technology*. [On-line]. 28(12). p. 125302. Available: http://stacks.iop.org/0957-0233/28/i=12/a=125302 [Jan. 15, 2018].

[13] F. K. Skinner, Y. Rotenberg, and A. W. Neumann. (1989, Jun.) "Contact angle measurements from the contact diameter of sessile drops by means of a modified axisymmetric drop shape analysis." *Journal of Colloid and Interface Science*. [On-line]. 130(1). pp. 25–34. Available: https://www.sciencedirect.com/science/article/pii/002197978990074X [Dec. 10, 2017].

[14] D. Y. Kwok, T. Gietzelt, K. Grundke, H.-J. Jacobasch, and A. W. Neumann. (1997, May.) "Contact angle measurements and contact angle interpretation. 1. contact angle measurements by axisymmetric drop shape analysis and a goniometer sessile drop technique." *Langmuir*. [On-line]. 13(10). pp. 2880–2894. Available: https://pubs.acs.org/doi/pdf/10.1021/la9608021 [Feb. 12, 2018].

[15] K. Uchino. (2008, Aug.) "Piezoelectric actuators 2006." *Journal of Electroceramics*. [On-line]. 20(3). pp. 301–311. Available: https://link.springer.com/article/10.1007/s10832-007-9196-1 [Feb. 12, 2018].

[16] *DROP SHAPE ANALYZER DSA100*, KRSS GmbH, 2017, [On-line]. Available: https://www.kruss-scientific.com/products/contact-angle/dsa100/drop-shape-analyzer-dsa100/ [Feb. 2, 2018].

[17] S. F. Chini and A. Amirfazli. (2011, Sep.) "A method for measuring contact angle of asymmetric and symmetric drops." *Colloids and Surfaces A: Physicochemical and Engineering Aspects*. [On-line]. 388(1). pp. 29–37. Available: https://doi.org/10.1016/j.colsurfa.2011.08.001 [Jan. 20, 2018].

[18] A. F. Stalder, T. Melchior, M. Mller, D. Sage, T. Blu, and M. Unser. (2010, Jul.) "Low-bond axisymmetric drop shape analysis for surface tension and contact angle measurements of sessile drops." *Colloids and Surfaces A: Physicochemical and Engineering Aspects*. [On-line]. 364(1). pp. 72–81. Available: https://www.sciencedirect.com/science/article/pii/S0927775710002761 [Nov. 14, 2017].

[19] O. I. del Ro and A. W. Neumann. (1997, Dec.) "Axisymmetric drop shape analysis: Computational methods for the measurement of interfacial properties from the shape and dimensions of pendant and sessile drops." *Journal of Colloid and Interface Science*. [On-line]. 196(2). pp. 136–147. Available: https://doi.org/10.1006/jcis.1997.5214 [Nov. 14, 2017].

[20] K. Y. Law and H. Zhao, *Contact Angle Measurements and Surface Characterization Techniques*. Cham: Springer International Publishing, 2016, pp. 7–34.